Using nano-QSAR to predict the cytotoxicity of metal oxide nanoparticles

Tomasz Puzyn[1,2], Bakhtiyor Rasulev[1], Agnieszka Gajewicz[1,2], Xiaoke Hu[3], Thabitha P. Dasari[3], Andrea Michalkova[1], Huey-Min Hwang[3], Andrey Toropov[4], Danuta Leszczynska[5] and Jerzy Leszczynski[1]*

It is expected that the number and variety of engineered nanoparticles will increase rapidly over the next few years[1], and there is a need for new methods to quickly test the potential toxicity of these materials[2]. Because experimental evaluation of the safety of chemicals is expensive and time-consuming, computational methods have been found to be efficient alternatives for predicting the potential toxicity and environmental impact of new nanomaterials before mass production. Here, we show that the quantitative structure–activity relationship (QSAR) method commonly used to predict the physicochemical properties of chemical compounds can be applied to predict the toxicity of various metal oxides. Based on experimental testing, we have developed a model to describe the cytotoxicity of 17 different types of metal oxide nanoparticles to bacteria *Escherichia coli*. The model reliably predicts the toxicity of all considered compounds, and the methodology is expected to provide guidance for the future design of safe nanomaterials.

Metal oxides are an important group of engineered nanoparticles, because they are widely used in cosmetics and sunscreens, self-cleaning coatings and textiles. Other applications include their use as water-treatment agents and as materials for solar batteries and more recent automobile catalytic converters[2]. However, it has been shown recently that nanosized particles of these oxides (but not their macro or micro counterparts) are toxic to some organisms[3]. It is therefore possible that sunscreens that contain these particles may be more hazardous than the UV radiation they protect against, and that the use of some solar batteries may have a higher environmental risk than carbon dioxide emission from conventional energy sources. Developing rapid methods for predicting the toxic behaviour and environmental impact of these nanoparticles is therefore important and timely.

According to the QSAR paradigm, if the molecular parameters (known as molecular descriptors) have been calculated for a group of compounds, but experimental data on the activity of those compounds are available for only part of the group, it is possible to interpolate the unknown activity of the other compounds from the molecular descriptors using a suitable mathematical model. Depending on the type of experimental data, QSAR can predict the physical and chemical properties or a vast range of activities and toxic influences of new compounds[2]. Previously, we have developed QSAR for use with nanomaterials (nano-QSAR) to predict their solubility[4], n-octanol/water partition coefficient[4] and Young's modulus[5]. Here, we apply nano-QSAR to predict the toxicity of nanoparticles. We have developed and validated a model to describe the relationship between the structures of 17 metal oxides and their cytotoxicity to *E. coli* cells. Based on this model and experimental data[6], we have hypothesized the most probable mechanism for the cytotoxicity of these nanoparticles. We investigated this cytotoxicity in bacteria, because although they are single-celled organisms, they can be used to evaluate the cytotoxicity of higher organisms. Indeed, because of their metabolic versatility, bacteria are considered an excellent ecological indicator for evaluating the persistence and impact of xenobiotic chemicals on environmental health and ultimately human health[6]. Furthermore, differences in the activity of individual oxides can be useful in dental applications, where they are used as antibacterial agents. Also, because bacteria, as decomposers, play an important role in natural ecosystems, the uncontrolled emission of highly bacteriotoxic substances may disrupt the natural balance and create unpredictable effects in the environment[7].

The nano-QSAR model was based on experimental data gathered in our laboratory for 17 metal oxide nanoparticles. The number of compounds, from the QSAR viewpoint, is small, but it allows the construction of a predictive model. Examples of classic QSAR studies successfully performed based on even smaller sets of compounds have been published elsewhere[8].

Based on the toxicity data and structural descriptors, we developed a simple but statistically significant ($F = 45.4$, $P = 0.0001$) nano-QSAR equation, using only one descriptor to successfully predict the cytotoxicity (denoted EC_{50}—the effective concentration of a compound that brings about a 50% reduction in bacteria viability) of the metal oxide nanoparticles:

$$\log(1/EC_{50}) = 2.59 - 0.50 \cdot \Delta H_{Me+} \qquad (1)$$

The descriptor ΔH_{Me+} represents the enthalpy of formation of a gaseous cation having the same oxidation state as that in the metal oxide structure:

$$Me(s) \rightarrow Me^{n+}(g) + n \cdot \bar{e}\Delta H_{Me+} \qquad (2)$$
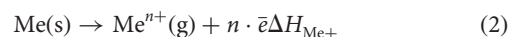
A complete list of the calculated molecular descriptors and details on the QSAR modelling procedure, including splitting for a training and validation set, data pre-processing, the method of modelling, internal validation, measuring goodness-of-fit and robustness, external validation of predictive ability and applicability domain, are described in Supplementary Sections 2.4–2.6.

Table 1 presents experimental and predicted data related to the toxicity of the studied nanomaterials in terms of EC_{50}. The predicted

[1]Interdisciplinary Nanotoxicity Center, Department of Chemistry and Biochemistry, Jackson State University 1400 Lynch Street, Jackson, Mississippi 39217-0510, USA, [2]Laboratory of Environmental Chemometrics, Faculty of Chemistry, University of Gdańsk, Sobieskiego 18, 80-952 Gdańsk, Poland, [3]Interdisciplinary Nanotoxicity Center, Department of Biology, Jackson State University, 1400 Lynch Street, Jackson, Mississippi 39217-0940, USA, [4]Instituto di Ricerche Farmacologiche Mario Negri, 20156, Via La Masa 19, Milano, Italy, [5]Interdisciplinary Nanotoxicity Center, Department of Civil and Environmental Engineering, Jackson State University, 1325 Lynch Street, Jackson, Mississippi 39217-0510, USA. *e-mail: jerzy@icnanotox.org

Table 1 | Structure and toxicity data.

Metal oxide	Descriptor ΔH_{Me+} (kcal mol^{-1})	Leverage value, h	Observed log 1/EC$_{50}$ (mol l^{-1})	Predicted log 1/EC$_{50}$ (mol l^{-1})	Residuals	Set
ZnO	662.44	0.33	3.45	3.30	0.15	T
CuO	706.25	0.29	3.20	3.24	−0.04	T
V$_2$O$_3$	1,097.73	0.11	3.14	2.74	0.40	V_1
Y$_2$O$_3$	837.15	0.21	2.87	3.08	−0.21	T
Bi$_2$O$_3$	1,137.40	0.10	2.82	2.69	0.13	T
In$_2$O$_3$	1,271.13	0.10	2.81	2.52	0.29	T
Sb$_2$O$_3$	1,233.06	0.10	2.64	2.57	0.07	V_1
Al$_2$O$_3$	1,187.83	0.10	2.49	2.63	−0.14	T
Fe$_2$O$_3$	1,408.29	0.13	2.29	2.35	−0.06	T
SiO$_2$	1,686.38	0.26	2.20	1.99	0.21	T
ZrO$_2$	1,357.66	0.11	2.15	2.41	−0.26	V_1
SnO$_2$	1,717.32	0.28	2.01	1.95	0.06	T
TiO$_2$	1,575.73	0.19	1.74	2.13	−0.39	T
CoO	601.80	0.38	3.51	3.38	0.13	V_2
NiO	596.70	0.39	3.45	3.38	0.07	V_2
Cr$_2$O$_3$	1,268.70	0.10	2.51	2.52	−0.01	V_2
La$_2$O$_3$	1,017.22	0.13	2.87	2.85	0.02	V_2

The critical value of h is 0.6.

EC$_{50}$ values were calculated using a single descriptor, ΔH_{Me+}. The nanomaterials in the training set (used to develop the QSAR equation) are denoted by T, those in the validation sets by V_1 and V_2. The leverage value h (acceptable if not higher than 0.6) indicates deviations of the structure of the compound from those used for the QSAR development. The data in Table 1 indicate that ZnO, CuO, NiO and CoO nanoparticles exhibit the highest cytoxicity to the bacteria, with TiO$_2$ nanoparticles being the least toxic.

Our observations parallel the results of previous studies. For instance, Heinlaan and colleagues[9] pointed out that the toxicity of three oxides (both nano and bulk) to the Gram-negative bacteria *Vibrio fischeri* increased as follows: TiO$_2$ < CuO < ZnO. Moreover, it was shown that the toxicity of nanosized oxides was much higher than their bulk counterparts. In a similar study, Adams and colleagues[10] noticed that the cytotoxicity of ZnO nanoparticles to both Gram-positive *Bacillus subtilis* and Gram-negative *E. coli* was significantly greater than that for TiO$_2$ nanoparticles. In contrast to our results, they observed very low toxicity from SiO$_2$, even lower than that found for TiO$_2$. Interestingly, they also revealed that particle size did not affect antibacterial activity. Similar sizes of aggregated particles were observed in water suspension, regardless of the powder size.

In parallel to our experimental toxicity testing, we quantitatively calculated a set of 12 parameters that describe the variability in the structure of nanoparticles (Supplementary Section 2.1). The descriptors were calculated using the quantum-chemical PM6 method[11]. Because particle size does not influence toxicity in the studied size range, the selected descriptors predominantly reflect reactivity-related electronic properties.

Experts who attended the 2008 NATO workshop[12] (designed to evaluate the widescale implications of the use of nanomaterials on human health and the environment) proposed four possible mechanisms for nanoparticle toxicity: (i) the release of chemical constituents from nanomaterials; (ii) the size and shape of the particle, which produces steric hindrances or interferences with the important binding sites of macromolecules; (iii) the surface properties of the material, such as photochemical and redox properties; and (iv) the capacity of nanomaterials to act as vectors for the transport of other toxic chemicals to sensitive tissues. They concluded that once a nanoparticle enters a cell, toxicity could occur through one or a combination of these mechanisms[12].

Auffan and colleagues[13] suggested that the most important parameter controlling the *in vitro* cytotoxicity of metallic nanoparticles (that is, zero-valent metals, metal oxides) is their chemical stability, which is related to the dissolution of the particles (release of cations) and the catalytic properties and redox modifications of the surface.
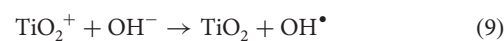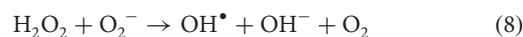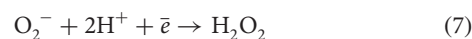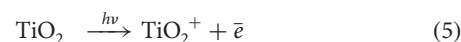
This is consistent with the first and third mechanisms proposed by the NATO experts. Moreover, the release of cations can occur by simple breaking of chemical bonds in the crystal lattice (without changing the oxidation state of the metal) or by redox reactions with the molecules in the biological media. In the latter case, the release of ions is often accompanied by the generation of reactive oxygen species (ROS), such as superoxide (O$_2^-$) and hydroxyl radicals (OH$^\bullet$). The observed toxicity can be induced by the released cations themselves, ROS or both[7,13].

Other groups[14,15] have observed that ionic silver (Ag$^+$) released from zero-valent silver nanoparticles induces oxidative stress following the generation of ROS. Auffan and colleagues[16] demonstrated that the release of Fe^{3+} cations from the metal surface was accompanied by ROS formation, according to the Fenton reaction:

$$Fe + O_2 + 2H^+ \rightarrow Fe^{2+} + H_2O_2 \qquad (3)$$

$$Fe^{2+} + H_2O_2 \rightarrow Fe^{3+} + OH^\bullet + OH^- \qquad (4)$$
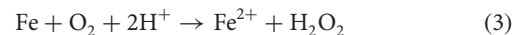
Heinlaan and colleagues[9], in a series of experiments, noticed that bio-available metal ions (detached from the surface) were responsible for the toxicity of ZnO and CuO in *V. fisheri* bacteria. For the case of insoluble CuO, the bioavailability of metal ions from nanoparticles was reported to be much higher than the bioavailability of ions from the bulk. Thus, CuO in its nano form was remarkably more 'soluble'. The solubilization of metal ions and generation of ROS may be increased by intimate contact of a nanoparticle with a cell membrane.

The potential impact of the reactive surface on the cytotoxicity of metal oxides may be illustrated by the redox instability of the CeO$_2$ surface[13] and the photocatalytic properties of TiO$_2$ (refs 7,17). In the former case, ROS may be generated from the fast valence exchange between Ce^{3+} and Ce^{4+}, whereas for TiO$_2$, ROS are produced in the presence of UV radiation[7,17]:

$$TiO_2 \xrightarrow{h\nu} TiO_2^+ + \bar{e} \qquad (5)$$

$$\bar{e} + O_2 \rightarrow O_2^- \qquad (6)$$

$$O_2^- + 2H^+ + \bar{e} \rightarrow H_2O_2 \qquad (7)$$

$$H_2O_2 + O_2^- \rightarrow OH^\bullet + OH^- + O_2 \qquad (8)$$

$$TiO_2^+ + OH^- \rightarrow TiO_2 + OH^\bullet \qquad (9)$$

Moreover, Daoud and colleagues[18] demonstrated that TiO_2 nanoparticles, in the absence of light, have reduced toxicity, suggesting that TiO_2 without UV radiation behaves in the same way as other metal oxides.

Our results indicate that ΔH_{Me+} can be utilized as an efficient descriptor of the chemical stability of metal oxides and, therefore, their cytotoxicity in *E. coli in vitro* tests. During the development of the model, we tested various parameters that were, in some cases, more interpretative than ΔH_{Me+}. The tests included ΔH_L (lattice energy), which describes the dissolution of nanoparticles without oxidation or reduction of the cation, and the electronic properties (energies of the highest occupied and the lowest unoccupied molecular orbitals) of the oxides, which describe their redox properties. In all these tests, the correlation between the tested descriptors and cytotoxicity was unsatisfactory (Supplementary Section 2.1).

However, the ΔH_{Me+} descriptor combines both types of mechanisms responsible for the cytotoxicity of the oxides. It is closely related to the lattice energy, because ΔH_L represents the enthalpy of the reaction:

$$a \cdot Me^{n+}(g) + b \cdot O^{2-}(g) \rightarrow Me_aO_b(s) \qquad \Delta H_L \qquad (10)$$
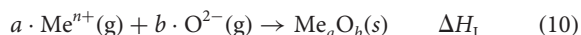
Negative values of the lattice energy increase with increasing cation charge (n). Similarly, positive values of ΔH_{Me+} increase with increasing charge (Table 1). Thus, the release of cations Me^{n+} having smaller charge is more energetically favourable than the release of cations with larger n. This explains why the toxicity of the studied oxides decreases in the following order: $Me^{2+} > Me^{3+} > Me^{4+}$. In addition, ΔH_{Me+} is also related to the sum of the ionization potentials of a given metal, because the formation of Me^{n+} cations requires sublimation followed by ionization reactions. Thus, it can be calculated as

$$\Delta H_{Me+} = \Delta H_S + \sum_{i=1}^{n} IP_i \qquad (11)$$

where ΔH_S is the enthalpy of sublimation and IP_i represents the nth ionization potentials of the metal. Obviously, much more energy is required to detach four electrons than three (or two) to form the appropriate cations.

Interestingly, the selected descriptor, ΔH_{Me+}, is not related to the size of the studied nanoparticles. This fact confirms our initial assumption, based on the results of ref. 10, that for a series of metal oxide nanoparticles of similar size, size is not a critical factor in determining variation in toxicity.

A plot of experimentally determined versus predicted log values of $1/EC_{50}$ is presented in Fig. 1. The straight green line represents perfect agreement between experimental and calculated values. The agreement between the observed toxicity values and those predicted by the nano-QSAR model is satisfactory for the metal oxides from the training set (squares) and those from the validation sets (triangles). The results for the statistics of the model (Supplementary Section 2.5) were obtained as follows: squared regression coefficient, $R^2 = 0.85$; cross-validated regression coefficient, $Q^2_{CV} = 0.77$; externally validated regression coefficient $Q^2_{ext} = 0.83$; root-mean-square error of calibration (RMSEC) = 0.20, of cross-validation (RMSECV) = 0.24, and of external prediction (RMSEP) = 0.19.

No-one should expect perfect agreement between observed and predicted data for experimentally tested toxicity[19]. According to the proposed reference criteria, the difference between R^2 and Q^2 should not exceed 0.3 (ref. 20). Moreover, Kubinyi[21] has recommended that $R^2 \geq 0.81$ for *in vitro* data and $R^2 \geq 0.64$ for *in vivo* data can be regarded as good. As our model fulfils these criteria
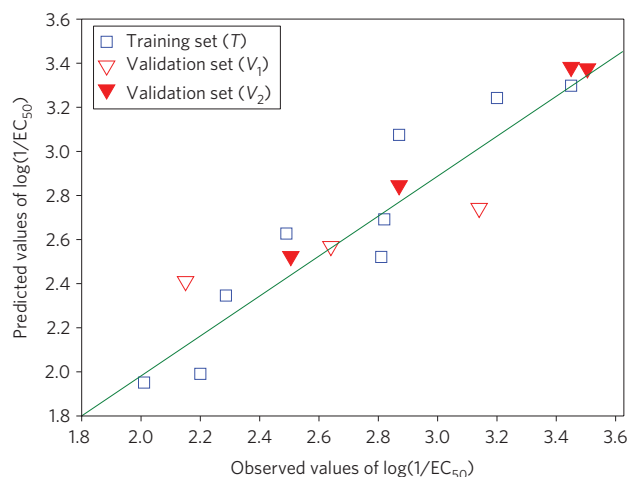
Figure 1 | Plot of experimentally determined (observed) versus predicted log values of $1/EC_{50}$. The straight line represents perfect agreement between experimental and calculated values. Squares represent values predicted for the metal oxides from the training set; triangles represent data calculated for metal oxides from the validation sets. The distance of each symbol from the green line corresponds to its deviation from the related experimental value.

and also positively passes internal and external validation (Supplementary Sections 2.5 and 2.6), it can be applied to predict the toxicity of new, untested oxides.

However, reliable predictions could only be performed within the optimum prediction space (so-called applicability domain) of the model. All the studied compounds were located within the optimum prediction space of the model (Supplementary Sections 2.5 and 2.6). We noticed that predictivity was satisfied even for CoO, the toxicity of which ($\log 1/EC_{50} = 3.51$) slightly exceeds the toxicity range covered by the training compounds ($3.45 > \log 1/EC_{50} > 1.74$). Thus, the model can be applied for predicting the toxicity of any other metal oxides, if their structures are not substantially different from the training set (that is, their calculated leverage values h should not be higher than 0.6).

In conclusion, based on a large number of metal oxide nanoparticles, the present study combines experimental testing and computational modelling methodologies to study the cytotoxicity of metal oxide nanoparticles in *E. coli*. We have successfully developed an interpretative nano-QSAR model that reliably predicts toxicity and provides the foundations for theoretical evaluation of the toxicity of untested nanomaterials, particularly metal oxides. Finally, we have formulated a hypothesis that mechanistically explains differences in toxicity between individual oxides.

Methods

Empirical toxicity testing. All 17 nanosized metal oxides (Table 1), with sizes ranging from 15 to 90 nm, were purchased from Sigma-Aldrich. *E. coli* (Migula) Castellani & Chalmers (ATCC#25254) strain was prepared at 37 °C overnight using Luria-Bertani (LB) broth. The cultures were centrifuged at 3,220*g* for 10 min and resuspended in sterilized physiological saline. Bacteria density was adjusted to (0.5×10^9)–(1.66×10^9) bacteria per ml as determined by colony forming unit (CFU) counting on LB petri dishes.

The cytotoxicity of the nanoparticles was expressed in terms of the logarithmic values of molar $1/EC_{50}$ (the effective concentration of a given oxide that reduces bacterial viability by 50%). Bacterial heterotrophic mineralization of glucose was also used to determine the metabolic rate of selected samples and was measured as follows. After being washed three times with physiological saline, 100 μl of *E. coli* suspensions were added to 10–20 ml of distilled water (control) or 10–20 ml of nanoparticle/distilled water solution at nominal concentrations of 200, 400 and 600 mg l⁻¹, respectively. To ensure dispersal, the stock solutions were prepared at a concentration of 1.2 g l⁻¹ with sonication treatment (FS30 ultrasonic system, Fisher Scientific) at 25 °C for 20 min. They were sonicated again for 10 min just before commencement of the exposure experiments. The control and experimental groups

were then agitated for 2 h at 150 r.p.m. A mineralization count of $^{14}CO_2$ released during metabolic respiration of radiolabelled UL-^{14}C D-glucose dissolved in ethanol (S.A. 2.48 mCi mmol^{-1}, Sigma) was conducted following the 2 h incubation period. At time zero, the Pyrex milk dilution bottle was sealed with a silicone stopper and a centre well containing a folded filter paper soaked with 0.7 ml β-phenylethylamine for CO_2 trapping. Trapping occurred overnight (8–12 h) after injection with 1M H_2SO_4 at the end of 2 h incubation. The filter papers were then removed and placed in 20 ml scintillation vials containing 8 ml Ultima Gold scintillation fluid (Packard) and counted with a liquid scintillation analyser (Packard Instrument, model TR 1600). Data were calculated from DPM (disintegrations per minute) readings to compute percent mineralizations[6].

The 13 nanoparticles, including those for which toxicity data were taken from our previous paper[6] (ZnO, CuO, Al₂O₃, Fe₂O₃, SnO₂, TiO₂) and those tested in Batch I (V₂O₃, Y₂O₃, Bi₂O₃, In₂O₃, Sb₂O₃, SiO₂, ZrO₂), were split into two sets, training set (T) and validation set (V_1) (Table 1), ensuring that the points from V_1 were evenly distributed within the range of toxicity of the training set compounds (T). Three compounds tested in Batch II (CoO, NiO, Cr₂O₃) and La₂O₃ were also then included in a validation set (V_2). For a detail justification of the splitting procedure please see Supplementary Section 2.2. Training set T was later used to develop the QSAR model. The toxicity of Batch II was tested after the nano-QSAR model had been developed. We used the validation set ($V_1 + V_2$) for external validation of the performance of the model to correctly predict the toxicity of novel oxides that had not previously been involved in the model's development.

To ensure that there was no systematic error between particular series of experiments as a result of variation in the laboratory conditions, in later experiments we repeated toxicity measurements for selected oxides that had been tested in the previous series. It should be emphasized, here, that this is the largest pool of experimental data on the toxicity of uniformly tested nanosized oxides, available from a single laboratory.

Computational part of the study. All quantum-mechanical calculations were performed using the PM6 method as implemented in MOPAC 2009[22]. Semi-empirical methods are much faster than quantum-mechanical *ab initio* and density functional theory (DFT) calculations. Semi-empirical methods allow calculations of larger systems to be carried out, but their accuracy is often disputed[23]. It is worth noting, however, that the PM6 approach, which uses a novel parameterization of the previously used PM3 Hamiltonian, delivers very accurate results comparing to DFT[24]. From a quantum-mechanical point of view, calculations for nanoparticles with a size of 15–90 nm (as in the experiments) were not feasible (the systems are too large), so it was necessary to maximally simplify the structural models used to calculate the descriptors. We calculated the descriptors using smaller metal oxide fragments (clusters) of the same size for all nanoparticles and one descriptor, based on the characteristics of the considered metal atoms (Supplementary Section 2.1).

For the modelling, we applied the multiple regression method combined with a genetic algorithm (GA-MLR). The GA was used to select the optimal combination of the previously calculated structural descriptors, to be utilized in the final model (Supplementary Section 2.4). We carried out calculations with the PLS Toolbox[25] and the Statistics Toolbox for MATLAB[26].

References

1. USEPA. *Economic Analysis of the Proposed Change in Data Requirements Rule for Conventional Pesticides.* (US Environmental Protection Agency, 2004).
2. Puzyn, T., Leszczynska, D. & Leszczynski, J. Toward the development of 'Nano-QSARs': advances and challenges. *Small* **5,** 2494–2509 (2009).
3. Dreher, K. L. Health and environmental impact of nanotechnology: toxicological assessment of manufactured nanoparticles. *Toxicol. Sci.* **77,** 3–5 (2004).
4. Toropov, A. A., Leszczynska, D. & Leszczynski, J. Predicting water solubility and octanol water partition coefficient for carbon nanotubes based on the chiral vector. *Comput. Biol. Chem.* **31,** 127–128 (2007).
5. Toropov, A. A. & Leszczynski, J. A new approach to the characterization of nanomaterials: predicting Young's modulus by correlation weighting of nanomaterials codes. *Chem. Phys. Lett.* **433,** 125–129 (2007).
6. Hu, X., Cook, S., Wang, P. & Hwang, H. M. *In vitro* evaluation of cytotoxicity of engineered metal oxide nanoparticles. *Sci. Total Environ.* **407,** 3070–3072 (2009).
7. Neal, A. L. What can be inferred from bacterium–nanoparticle interactions about the potential consequences of environmental exposure to nanoparticles? *Ecotoxicology* **17,** 362–371 (2008).
8. Puzyn, T., Mostrag, A., Falandysz, J., Kholod, Y. & Leszczynski, J. Predicting water solubility of congeners: chloronaphthalenes—a case study. *J. Hazard. Mater.* **170,** 1014–1022 (2009).
9. Heinlaan, M., Ivask, A., Bilnova, I., Dubourguier, H. C. & Kahru, A. Toxicity of nanosized and bulk ZnO, CuO and TiO₂ to bacteria *Vibrio fischeri* and crustaceans *Daphnia magna* and *Thamnocephalus platyurus*. *Chemosphere* **71,** 1308–1316 (2008).
10. Adams, L. K., Lyon, D. Y. & Alvarez, P. J. Comparative eco-toxicity of nanoscale TiO₂, SiO₂, and ZnO water suspensions. *Water Res.* **40,** 3527–3532 (2006).
11. Stewart, J. J. P. Optimization of parameters for semiempirical methods. V: modification of NDDO approximations and application to 70 elements. *J. Mol. Model.* **13,** 1173–1213 (2007).
12. Linkov, I. *et al.* Emerging methods and tools for environmental risk assessment, decision-making, and policy for nanomaterials: summary of NATO Advanced Research Workshop. *J. Nanopart. Res.* **11,** 513–527 (2009).
13. Auffan, M., Rose, J., Wiesner, M. R. & Bottero, J. Y. Chemical stability of metallic nanoparticles: a parameter controlling their potential cellular toxicity *in vitro*. *Environ. Pollut.* **157,** 1127–1133 (2009).
14. Kim, J. S. *et al.* Antimicrobial effects of silver nanoparticles. *Nanomed. Nanotechnol. Biol. Med.* **3,** 95–101 (2007).
15. Pal, S., Tak, Y. K. & Song, J. M. Does the antibacterial activity of silver nanoparticles depend on the shape of the nanoparticle? A study of the gram-negative bacterium *Escherichia coli*. *Appl. Environ. Microbiol.* **73,** 1712–1720 (2007).
16. Auffan, M. *et al.* Relation between the redox state of iron-based nanoparticles and their cytotoxicity toward *Escherichia coli*. *Environ. Sci. Technol.* **42,** 6730–6735 (2008).
17. Burello E. & Worth, A. P. A theoretical framework for predicting the oxidative stress potential of oxide nanoparticles. *Nanotoxicology* doi:10.3109/17435390.2010.502980 (15 July 2010).
18. Daoud, W. A., Xin, J. H. & Zhang, Y. H. Surface functionalization of combined bactericidal activities. *Surf. Sci.* **599,** 69–75 (2005).
19. Cronin, M. T. D. & Schultz, T. W. Pitfalls in QSAR. *J. Mol. Struct.* **622,** 39–51 (2003).
20. Eriksson, L. *et al.* Methods for reliability and uncertainty assessment and for applicability evaluations of classification- and regression-based QSARs. *Environ. Health Perspect.* **111,** 1361–1375 (2003).
21. Kubinyi, H. *Methods and Principles in Medicinal Chemistry* Vol. 1 (eds Mannhold, R., Kroogsgard-Larsen, P. & Timmerman, H.) (VCH, 1993).
22. Stewart, J. J. P. MOPAC2009 (Stewart Computational Chemistry, 2009).
23. Jensen, F. *Introduction to Computational Chemistry* (Wiley, 1999).
24. Puzyn, T., Suzuki, N., Haranczyk, M. & Rak, J. Calculation of quantum-mechanical descriptors for QSPR at the DFT level: is it necessary? *J. Chem. Inf. Model.* **48,** 1174–1180 (2008).
25. PLS_Toolbox, ver. 4.2.1 (Eigenvector Research, 2007).
26. MATLAB_7.6, available at http://www.mathworks.com (MathWorks, 2008).

Author contributions

X.H., T.P.D. and H-M.H. carried out empirical testing of the cytotoxicity of the metal oxides to *E. coli*. A.M. designed molecular clusters for calculations. T.P., B.R., A.G., A.M., A.T., D.L. and J.L. performed quantum-mechanical calculations, selected the optimal structural descriptors, developed and validated the nano-QSAR model and discussed the results.

Additional information

The authors declare no competing financial interests. Supplementary information accompanies this paper at www.nature.com/naturenanotechnology. Reprints and permission information is available online at http://npg.nature.com/reprintsandpermissions/. Correspondence and requests for materials should be addressed to J.L.